HEXOKINASE 1 Glycolytic Action Fuels Post-Germinative Seedling Growth

Ashwin Ganpudi[1], Andrés Romanowski[1], Karen J. Halliday[1]

1. Institute for Molecular Plant Sciences, School of Biological Sciences, University of Edinburgh, Edinburgh EH9 3BF, United Kingdom.

ORCID IDs: 0000-0002-9515-3899 (A.G.); 0000-0003-0737-2408 (A.R.); 0000-0003-0467-104X (K.J.H.)

Corresponding author:

Karen J. Halliday

Institute for Molecular Plant Sciences, School of Biological Sciences, University of Edinburgh, Edinburgh EH9 3BF, United Kingdom

+44-0131-651-9083

karen.halliday@ed.ac.uk

Abstract

HEXOKINASE 1 (HXK1) is an evolutionarily conserved glycolytic enzyme that has a separate nuclear glucose-sensor signalling function. In Arabidopsis, HXK1 mutant seedlings have a stunted growth defect, yet how this relates to HXK1 function remains inconclusive. We show that the HXK1-glycolytic pathway performs a fundamental role in catabolising seed reserves to fuel post-germinative cell division and expansion. This function is particularly important in dim light which delays the switch to photoautotrophic growth. RNAseq analysis reveals that HXK1 imposes strong repressive control on plastome gene expression, and regulates nuclear-encoded genes that drive energy-consuming processes. Earlier studies have implicated HXK1 sensor-signalling in the repression of *CAB2* and *CAA* gene expression by exogenous glucose. We show that over a wide range of irradiances this pathway is not operative in seedlings. Our study therefore defines a new operational model

for HXK1 action in catabolising carbon resources and tuning gene expression to optimize seedling growth.

Introduction

The first days of life are critical for plant survival. Successful seedling establishment relies on seed reserves to support emergence before the switch to photosynthetic growth. The endosperm of oil seed plants, such as Arabidopsis, contains mainly triacylglycerols (TAG) and storage proteins, which are mobilized during germination (***Baud et al., 2005; Penfield et al., 2006***). Several studies have highlighted the critical role for TAGs in gluconeogenic sugar production, which fuels post-germinative seedling growth (***Graham, 2008; Theodoulou and Eastmond, 2012***). When germination occurs in darkness, or dim light seedlings adopt a skotomorphogenic-type program where growth is largely confined to the seedling stem (hypocotyl), at the expense of seedling leaf (cotyledon) and root development. A large body of work has shown that members of the light regulated PHYTOCHROME INTERACTING FACTOR (PIF) gene family operate cooperatively to regulate skotomorphogenesis (***Gommers and Monte, 2018; Leivar and Monte, 2014; Chaiwanon et al., 2016***). This growth strategy allows seedlings to forage for light when occluded by soil, debris or vegetation cover. It is energy-conserving, as it restricts growth to one organ, reducing the pull-on finite seed reserves.

Following gluconeogenesis, glucose is either used as a building block for protein, fatty acid or cellulose production, or it is catabolized to generate energy for cellular metabolism and growth. A fundamental enzyme in this latter process is the evolutionarily conserved HEXOKINASE 1 (HXK1) that catalyses the first glycolytic step of glucose phosphorylation to generate glucose-6-phosphate (G6P) (***Cárdenas et al., 1998; Claeyssen and Rivoal, 2007***). In addition to its enzymatic role, Arabidopsis HXK1 is reported to have a conserved glucose activated signalling function where HXK1 operates in a nuclear-located complex with VACUOLAR H(+)-ATPase B1 (VHA-B1) and the 19S regulatory particle of proteasome subunit (RPT5B) (***Yanagisawa et al., 2003; Moore et al., 2003; Cho et al., 2007***). The

HXK1 complex was shown to be necessary for glucose-induced repression of *CHLOROPHYLL A/B BINDING PROTEIN 2* (*CAB2)* and *CARBONIC ANHYDRASE (CAA)*. ChIP-qPCR analysis indicated that at least for *CAB2* this transcriptional suppression was direct. This sugar-dependent, nuclear regulatory role of HXK1 was postulated to function during feedback inhibition of photosynthesis (***Moore et al., 2003; Cho et al., 2007***). Other reports have also implicated HXK1 in the transcriptional repression of developmental genes in response to exogenous sugar application (***Yang et al., 2013; Yu et al., 2013; de Jong et al., 2014; Hsu et al., 2014; Kunz et al., 2015***).

A prominent feature of the *glucose insensitive 2 (gin2)* mutant that lacks HXK1, is its diminutive seedling phenotype (***Moore et al., 2003; Cho et al., 2007***). Earlier work showing mutated catalytic domain constructs, $HXK1^{S177A}$ and $HXK1^{G104D}$, could complement the *gin2* seedling phenotype (**Moore et al., 2003**) suggested *gin2* stunting arose from impaired glucose-activated HXK1 signalling, and not HXK1 enzyme activity. However, several reports present data that are incongruous with this interpretation, so the precise role of HXK1 in seedlings remains unclear. Our study establishes that the HXK1-glycolytic pathway fulfils an important function in supporting early seedling growth. This is particularly important during light limited conditions that attenuate the switch to photoautotrophic growth. Under physiologically relevant conditions, glucose repression of the photosynthetic genes *CAB2 and CAA* does not require HXK1. Rather, HXK1 boosts the expression of genes involved in aerobic respiration and energy-consuming processes and strongly represses the Branched Chain Amino Acid (BCAA) alternative respiratory pathway and the plastome. Thus, HXK1 plays a central role not just in glycolysis but in coordinating the transcriptional regulation of cellular metabolism in developing seedlings.

Results

HXK1 supports post germination growth in darkness and low light. The *gin2* mutant was previously reported to have impaired hypocotyl growth in low light and nutrient conditions (***Moore et al., 2003; Cho et al., 2007***). We therefore wanted to establish the

fluence rate range in which HXK1 operates. This was assessed by growing HXK1 mutants *gin2* (Ler) and *hxk1-3* (Col) in darkness or increasing irradiances of continuous white light. Our data show both *gin2* and *hxk1-3* exhibit shorter hypocotyls than their respective isogenic wild types in darkness and low fluence rates (***Figure 1A***). Likewise, *gin2* and *hxk1-3* cotyledon expansion is impaired at low, but not high fluence rates (***Figure 1B,C***). This indicates that HXK1 has an important role in supporting seedling growth in darkness and light limiting conditions.

In nature, plants do not commonly experience uninterrupted continuous light, so we wanted to establish whether the *gin2* / *hxk1-3* seedling phenotypes were evident in photoperiodic conditions. We found that this was indeed the case in Short Days (SD), but not in Long Days (LD). However, by lowering the fluence rate from 100 to 5 µmol m^{-2} s^{-1} in LD we were able to restore the *gin2* / *hxk1-3* short hypocotyl phenotype (***Figure1-figure supplement 1***). These data illustrate that HXK1 is required for hypocotyl extension in short photoperiods or in LDs when access to light is restricted.

We next quantified hypocotyl epidermal cell length and number to establish the basis of the hypocotyl defect in *gin2.* On day 4 *gin2* had less elongated cells, and this was most noticeable in the upper elongation region (34% decrease) (***Figure 1D***). We also established that on day 4 and day 14, after growth cessation, *gin2* hypocotyls had fewer epidermal cells than wild type (***Figure 1E***). Interestingly, we also observed that in darkness *gin2* mutants had 55% higher levels of glucose than wild type (***Figure 1F***), which is indicative of impaired HXK1 catalytic function. Supporting this notion, G6P but not glucose was able to rescue the *gin2* short etiolated hypocotyl phenotype (***Figure 1G***). Application of sodium pyruvate (the salt of glycolytic end product pyruvate) was nearly as effective as G6P (***Figure1-figure supplement 2***). Thus, our data imply HXK1 catalytic activity has an important function in supporting cell proliferation and expansion in the seedling hypocotyl under light-restricted conditions.

RNA-seq reveals role for HXK1 in nutrient resource management. To gain an appreciation of how HXK1 influences gene expression we performed RNA-seq on 4-day-old

etiolated WT and *gin2* seedlings. This data revealed that 2353 genes were mis-regulated (± 1.5 FC) in *gin2* vs wild type, with 1276 genes down regulated, and 1077 upregulated (***Figure 2-figure supplement 1***, ***Figure 2-source data 1***). Amongst the downregulated subset we noted a predominance of energy demanding pathways, for instance over-represented GO terms included ribosome biogenesis, protein synthesis, translation, ATP driven cytoskeletal motor proteins, microtubules (kinesins) and microfilaments (myosins) (***Figure 2A***). Cytoskeletal motor proteins require microtubules and microfilaments to mobilize the organization of various cytoskeletal arrays during cell division, cell expansion and cell growth in plant tissues (***Hashimoto, 2015***). Indeed, several *CYCLIN (CYC)* genes that regulate cell cycle progression and cell wall remodelling *XYLOGLUCAN ENDOTRANSGLUCOSYLASE / HYDROLASE (XTH)* genes are also down-regulated in *gin2* (***Figure 2-figure supplement 2***). Collectively, these observations are consistent with the *gin2* phenotype that is characterized by a reduction of cell division, expansion and growth (***Figure 1D,E***).

Amongst the upregulated transcript subset, enriched processes include abscisic acid and auxin response pathways, water and photoperception responses. However, by far the most prominent of these categories is of the branched chain amino acids (BCAA), leucine (Leu), isoleucine (Ile) and valine (Val) (***Figure 2B***). BCAA degradation is an evolutionary conserved mitochondrial pathway induced by intense carbon starvation (***Binder, 2010; Hildebrandt et al., 2015***) (***Figure 2C***). Oxidation of BCAAs directly feeds electrons into the electron transport chain. The carbon skeletons are further converted to precursors of the tricarboxylic acid (TCA) cycle through a series of biochemical steps for subsequent ATP production. Hence, enhanced regulation of this pathway in *gin2* could help support cellular respiration and subsequently energy production, as glycolysis is impaired.

Our qRT-PCR data show that 0.5% glucose application suppresses the expression of BCAA catabolic pathway genes (*BRANCHED-CHAIN AMINO ACID TRANSAMINASE 2 (BCAT2), DARK INDUCIBLE 2 (DIN2), THIAMIN DIPHOSPHATE-BINDING FOLD PROTEIN (THDP), ISOVALERYL-COA-DEHYDROGENASE (IVD)* and *3-METHYLCROTONYL-COA CARBOXYLASE subunits (MCCA and MCCB)* in both wild type and *gin2* seedlings (***Figure***

2D). Thus, glucose suppression of *BCAA* genes does not require HXK1. In contrast, G6P application was ineffective in wild type, but fully restored the elevated expression of *BCAA* genes in *gin2* to wild type levels (***Figure 2D***). As G6P can substitute for HXK1 deficiency this suggests that reduced glycolysis in *gin2* leads to the activation of the BCAA pathway as an alternative energy source for respiration.

HXK1 represses the plastome in the dark. An interesting observation from our RNA-seq data is that HXK1 loss leads to a dramatic upregulation of 94% chloroplast-encoded and 24% mitochondrial genes in etiolated seedlings (***Figure 3A***). Chloroplastic genes represent the most highly upregulated category in *gin2*, suggesting HXK1 has an important role in global suppression of the chloroplast genome in darkness. This finding provided an opportunity to test whether HXK1 is also able to regulate non-nuclear genes through the G6P pathway. Here we chose to analyse the chloroplast-encoded *RNA POLYMERASE SUBUNIT* genes *RPOA, RPOB, RPOC1* and *RPOC2* that are required for chloroplast gene transcription. We found that G6P induced expression of *RPOA, RPOB, RPOC1* and *RPOC2* in both wild type and *gin2*. However, as transcript levels were already elevated in *gin2*, its G6P-induced response was attenuated (***Figure 3B***). These results suggest that while HXK1 most likely regulates these plastid genes through a G6P-dependent pathway, it is not the sole regulator. It is possible that HXK1 homologue HXK2 or the chloroplast located HXK3 operate redundantly with HXK1 to regulate these plastid genes. Collectively, these data provide genetic evidence that HXK1 regulates plastid-encoded as well as nuclear-encoded genes most likely by enzymatic catalysis of the first step in glycolysis that yields G6P.

HXK1 regulates a small subset of PIF-targets. Similar to *gin2* and *hxk1-3*, *pif* mutations can impair hypocotyl elongation in etiolated seedlings, and this effect is pronounced in the higher order *pifQ* mutant that lacks *PIF1, PIF3, PIF4* and *PIF5* (***Leivar et al., 2008; 2012***). We therefore wanted to establish the degree of overlap between the HXK1 and PIF regulated transcriptomes by comparing RNA-seq data from our study (4-day old etiolated *gin2* seedlings) and a published dataset (2-day old etiolated *pifQ* mutants) (***Pfeiffer et al., 2014***). In total, 4223 (± 1.5 FC) genes were misregulated in *pifQ*/wt compared to 2353 (± 1.5

FC) in *gin2*/Wt, with 748 common genes, which represents 11% of the total gene population, but 32% of HXK1-regulated genes (***Figure 3C***). Interestingly, like *gin2*, the *pifQ* transcriptome was enriched for BCAA catabolic pathway genes. However, while BCAA genes *BCAT2, DIN2, THDP, IVD, MCCA, MCCB* are elevated in *gin2*, they are severely suppressed in the *pifQ* mutant (***Figure 3-figure supplement 1***). As the promoters of these genes are not identified as PIF-bound in these conditions (***Pfeiffer et al. 2014; Zhang et al., 2013***), this suggests that the differences in *BCAA* gene expression in *pifQ* and *gin2* could reflect differences in their respective metabolic states.

Next, we examined the likelihood of HXK1-PIF cross-talk by identifying the common gene subset that are directly bound by PIFs based on ChIP-seq analysis (***Pfeiffer et al., 2014***). Interestingly, this subset represents only 4.6% of common genes, suggesting that potential cross-talk may be limited. By far the largest groups of genes were those upregulated by both HXK1 and PIFs which are predominantly involved in metabolism (***Figure 3-figure supplement 2***). In contrast, direct PIF targets that are HXK1-repressed are primarily transcription factors and hormone regulated genes. Shared genes include *PIL2 (PIF6)* and *LONG HYPOCOTYL IN FAR-RED* (*HFR1)*, two well characterized PIF-targets (***Pfeiffer et al., 2014; Zhang et al., 2013; Hornitschek et al., 2012***). Thus, we were keen to establish if these genes are regulated by the HXK1-G6P pathway. We found that *PIL2* expression is lower in *gin2*, and that G6P application can reduce expression to similarly low levels in wild type and *gin2* (***Figure 3D***). This data indicates that HXK1 can promote *PIL2* expression, but G6P suppresses *PIL2* levels independently of HXK1. On the other hand, *HFR1* expression appears to be repressed by the HXK1-G6P pathway (***Figure 3D***). Our analysis implies that PIFs and HXK1 both promote *PIL2* expression, but PIFs and HXK1-G6P have opposing roles in the regulation of *HFR1*.

HXK1 is functionally important under low light conditions. Our fluence response and short-day data (***Figure 1 and Figure 1-figure supplement 1***) illustrates that HXK1 loss curtails seedling growth in light limiting conditions as well as in darkness. Therefore, we were interested to establish if HXK1 was important for catabolizing photosynthesis-derived

glucose in low light. We found that G6P application enhanced *gin2* hypocotyl length in a dose-dependent manner with full restoration of *gin2* hypocotyl length occurring at a concentration of 5mM (0.125% w/v) G6P (***Figure 4A***). Likewise, application of sodium pyruvate is able to restore *gin2* seedlings to wild type dimensions (***Figure 4-figure supplement 1***). This confirms that as for dark conditions, HXK1 enzymatic function is important for supporting seedling growth in low irradiance light. The data also confirm that the 0.125% concentrations that we have used across experiments lie at the upper limit of the physiological range.

HXK1 does not mediate glucose-induced hypocotyl elongation. Earlier work has implicated HXK1 in glucose induced signalling, indeed the *gin2* mutant was identified in a glucose insensitive germination assay (***Moore et al., 2003***). However, HXK1 does not appear to control glucose-induced hypocotyl elongation, a response mediated by PIFs, and BRASSINAZOLE-RESISTANT 1 (BZR1) (***Stewart et al., 2011; Zhang et al., 2016***). In accord with these studies we have shown that (1%) glucose-mediated hypocotyl extension is greatly attenuated in the *pifQ* mutant but not in *gin2* which has a near wild type response (***Supplementary file 1***). In conditions that mimic the original *gin2* mutant screen, we can show that, as expected, 6% glucose blocks wild type seedling development, while *gin2* is unaffected. At these high glucose concentrations, like the wild type, *pifQ* fails to thrive (***Supplementary file 1***). These observations indicate that HXK1 and PIFs operate in distinct glucose-activated signalling pathways and that HXK1 is not the primary sensor for glucose activated hypocotyl elongation induced by exogenous glucose.

HXK1 does not suppress photosynthetic gene repression in seedlings. While our data show HXK1 enzymatic action supports post-germinative seedling growth, we wanted to establish if we could also find evidence for a glucose-activated HXK1 signalling function. Previous studies have implicated HXK1 signalling in glucose-mediated transcriptional suppression of the photosynthetic genes *CAB2* and *CARBONIC ANHYDRASE (CAA)* (***Moore et al., 2003; Cho et al., 2007***). Consistent with these earlier studies, we also observe glucose mediated suppression of *CAB2* and *CAA* expression in wild type seedlings,

and the severity of suppression is dose dependent (***Figure 4B***). Likewise, our data illustrate that HXK1 is required for glucose-suppression of *CAB2* and *CAA* expression, but only at the higher 1% concentration (and not 0.5% glucose). Application of G6P does not substantially change *CAB2* or *CAA* expression in either wild type or *gin2*, implying that in seedlings *CAB2* and *CCA* are not regulated by the HXK1-G6P pathway (***Figure 4B***). Rather, these photosynthetic genes are negatively regulated by an alternative HXK1-requiring pathway that is activated by exogenously applied glucose above a concentration threshold.

Given this finding we wanted to establish whether commonly applied glucose concentrations (0.5-2%) were compatible with or exceeded physiological levels (***Figure 4C***). This was accomplished by quantifying internal glucose levels in seedlings grown in SD under increasing light fluence rates: 100, 300 or 600 µmol $m^{-2}s^{-1}$ (referred to henceforth as 100, 300 and 600) and those grown in 100, and supplied with 0.5%, 1% or 2% exogenous glucose. We aimed to include seedlings grown at higher fluence rates (800µmol $m^{-2}s^{-1}$), but they photobleached and perished. In irradiances of 100, internal glucose was recorded at 0.4 mg/g FW and rose by 1.9-fold to 0.75 mg/g FW in seedlings grown at 600 (***Figure 4C***). In comparison, the exposure to the lowest dose (0.5%) increased internal glucose levels to 2.59 mg/g FW, which amounted to a 6.5-fold increase when compared to control (100) or 3.45-fold when compared to seedlings grown in 600. Application of 1% or 2% greatly surpasses the normal range of endogenous glucose levels in young seedlings. This data illustrates that even the lowest (0.5%) dose of glucose exceeds normal physiological levels by some margin (***Figure 4C***).

We then tested whether *CAB2* and *CAA* expression could be repressed in plants grown in increased light levels that generate physiological increases in glucose. We found that growth in 600 compared to 100 led to a small upregulation in *CAB2* in wild type but not in *gin2* (***Figure 4-figure supplement 2***). The response of *CAA* to increased fluence rates was relatively unchanged in both genotypes. This indicates that in our conditions, high light stimulates *CAB2* expression in a HXK1-dependent manner, however this response is very subtle.

As the above analysis was conducted in SD conditions that restrict the photosynthetic period, we extended this line of investigation to seedlings grown in long day (LD) photoperiods at a slightly warmer temperature to maximize photosynthetic potential. In LD (100), end-of-day seedling glucose levels were nearly two-fold higher than SD (100) but fell substantially below the 0.5% exogenous glucose dose (***Figure 4C,D***). We also recorded an incremental fall in glucose levels in 100, 600 and 800. Although we expect flux to glucose to be dynamic, the internal free-glucose pool is highly regulated (***Mengin et al., 2017***). Indeed, we found that end-of-day glucose levels decreased slightly with increased fluence rate (***Figure 4D***). Despite this we recorded a light dose dependent decrease in *CAB2* expression in both wild type and *gin2* (***Figure 4E***). As for SD, in LD *CAA* levels are relatively unchanged by light dose in wild type and *gin2*. Earlier studies have reported that *HXK1* transcript abundance is upregulated by glucose application (***Price et al., 2004; Yang et al., 2013; Kelly et al., 2017***). In both our SD and LD conditions we do not observe a fluence rate dependent regulation of *HXK1* transcript levels. Collectively our data illustrate that internal glucose levels do not appear to rise above the threshold that is required for HXK1-mediated repression of *CAB2* and *CAA* expression (***Figure 4E and Figure 4-figure supplement 2***). This indicates that in seedlings the glucose-activated HXK1 suppression of these photosynthetic genes may not operate.

Discussion

The glucose sensor HXK1 has been shown to function as a glycolytic enzyme, and a glucose-activated nuclear signalling component proposed to operate during seedling and adult developmental stages (***Moore et al., 2003; Cho et al., 2007***). Our study delineates an important glycolytic role for HXK1 in the emerging seedling. The *gin2* and *hxk1-3* mutations cause stunting in seedlings grown in darkness or low light conditions (***Figure1 A,B and Figure 1-figure supplement 1***). Quantification of cell number and dimensions reveal that HXK1 depletion restricts hypocotyl cell division and expansion (***Figure 1D,E***). The *gin2* mutant accumulated higher levels of glucose than the wild type, indicative of impaired HXK1 catalytic function (***Figure 1F***). Further, application of G6P (or sodium pyruvate), but not

glucose, restored *gin2* seedlings to wild type dimensions (***Figure 1G and Figure 1-figure supplement 2***). These data point to loss of HXK1 enzymatic function as the cause of *gin2* and *hxk1-3* seedling stunting. In etiolated seedlings, seed endosperm reserves are used to fuel hypocotyl elongation. Indeed, like HXK1 mutants, the glyoxylate cycle mutant, *isocitrate lyase (icl)* and the *phosphoenolpyruvate carboxykinase1 (pck1)* mutant, that blocks carbon export from the endosperm, also exhibit short hypocotyl phenotypes in the dark (***Eastmond et al., 2000; Penfield et al., 2004***). Our findings therefore indicate that HXK1 is an important component of the carbon respiratory machinery that supports post-germinative growth and this is particularly evident in light-limiting conditions. Lending further support to our findings, the catalytic activity of an ancestral type B KnHXK1, was recently shown to rescue the diminutive *gin2* adult phenotype (***Ulfstedt et al., 2018***).

HXK1 is known to regulate gene expression through both glucose-activated signalling and glycolysis-dependent pathways. Through RNA-seq analysis we established that in darkness HXK1 loss leads to altered expression of 2189 nuclear genes which represents 12% of the transcriptome. Just over half (54%) exhibited reduced expression in *gin2 vs* WT, a subset strongly enriched for energy demanding processes such as ribosome biogenesis, translation, motor activity and cytoskeleton-dependent transport (***Figure 2A***). In accordance with the reduction of cell division and expansion in *gin2* compared to wild type, we recorded a concomitant reduction in the expression of several core *CYC* and *XTH* genes (***Figure 1D,E and Figure 2-figure supplement 2***). In contrast, upregulated genes in *gin2* are strongly enriched for BCAA enzymes and to a lesser extent hormone response pathways (***Figure 2B***). Catabolism of the BCAA's, Ile, Leu and Val, is known to support respiration under carbohydrate-limiting conditions (***Binder, 2010; Hildebrandt et al., 2015***). Recent work has shown that the expression of BCAA pathway genes are directly activated in extended darkness by SnRK1 mediated S_1-bZIP signalling (***Pedrotti et al., 2018***; ***Baena-González et al., 2007***). Our data indicate that the enhanced expression of BCAA catabolism enzymes in *gin2* results from depleted HXK1-glycolytic signalling, as G6P application restores BCAA gene expression to wild type levels (***Figure 2D***). Interestingly, exogenous

glucose application represses BCAA gene expression in wild type, but also in *gin2*, indicating this glucose-mediated response does not require HXK1 (***Figure 2D***). Our results therefore show that BCAA gene expression is regulated through the HXK1-glycolytic pathway and when HXK1 is fully operational the BCAA carbon starvation-activated pathway is suppressed.

Remarkably, our RNA-seq analysis revealed that the majority (94%) of the chloroplast genome and 27% of mitochondrial genes were up-regulated in *gin2* (***Figure 3A***). This identifies an important novel function for HXK1 in the repression of mitochondrial and chloroplastic gene expression in darkness. Like the BCAA catabolic pathway genes, we showed that the chloroplast-encoded polymerase subunits *RPOA, RPOB, RPOC1* and *RPOC2* were also regulated by the HXK1 glycolytic pathway. However, in contrast to *BCAA* genes, G6P application enhanced polymerase subunit gene expression in wild type and to a lesser extent in *gin2*, suggesting HXK2 and/or the plastid localized HXK3, may operate redundantly with HXK1 in the regulation of these genes. Indeed, HXK1, HXK2, and particularly HXK3 have been implicated in the regulation of sugar-dependent retrograde signalling, whereby chloroplast gene expression imposes control on nuclear-encoded photosynthetic gene *LHCB1* (***Zhang et al., 2010***). Our data implies HXK genes operate redundantly to modulate chloroplastic gene expression and this occurs at least partly through the glycolytic pathway.

As the light regulated PIF transcription factors control skotomorphogenic growth, therefore we sought to establish the extent to which HXK1 and PIF mediated gene expression overlapped by comparing our RNA-seq data with published *pifQ* transcriptome data (***Pfeiffer et al. 2014; Zhang et al., 2013***). 32% of HXK1 controlled genes were also regulated by PIFs. BCAA pathway genes were amongst the highly enriched category of PIF-controlled pathways, but it seems that here PIFs act antagonistically with HXK1 by promoting *BCAA* gene expression (***Figure 3-figure supplement 1***). From the common gene-set we identified a smaller group of genes that are directly regulated by PIFs (***Zhang et al., 2013; Pfeiffer et al., 2014***). In this group, “PIF- and HXK1-induced genes” was the largest individual category,

which was strongly enriched for metabolic pathway genes (***Figure 3-figure supplement 2***). Direct PIF targets that were repressed by HXK1 contained a higher proportion of transcription factors and hormone genes. We established that *HFR1*, a gene that is transcriptionally activated by PIFs is repressed by the HXK1-G6P pathway (***Figure 3D***). This finding illustrates that carbon status can influence the expression of this key light signalling component. HFR1 action may therefore be governed by both the external light and internal metabolic environment.

Several studies have shown sugar application can control hypocotyl elongation, and that PIFs and BZR1 are important transcriptional modulators of this response (***Stewart et al., 2011; Zhang et al., 2016***). Our data and that of other labs (***Singh et al., 2017; Zhang et al., 2016; Simon et al., 2018***) suggest that HXK1 is not the primary effector. Instead the nutrient sensor Target Of Rapamycin (TOR) kinase is required for sugar induced stabilization of BZR1 protein and seedling growth (***Zhang et al., 2016***). Further, a recent study has shown the TOR-translation pathway, via ribosomal S6 kinase (S6K) and its substrate, ribosomal protein S6 (RPS6), is photoreceptor-activated during the switch to photomorphogenic seedling growth (***Chen et al., 2018***). Thus, it appears that TOR has a prominent role in integrating sugar and light sensory signals in the developing seedling.

To investigate more thoroughly the potential for HXK1 glucose signalling in seedlings we analysed photosynthetic genes *CAB2* and *CAA*, shown previously to be directly targeted by HXK1 following glucose activation (***Cho et al., 2007***). As for earlier reports, we showed that exogenously applied glucose inhibited *CAB2* and *CAA* expression in a HXK1-dependent manner, but there is a threshold glucose concentration (1%) over which HXK1 operates (***Figure 4B***). By measuring internal glucose levels, we established that the effective 1% glucose, and even lower 0.5% dose, both greatly exceed physiological levels under a range of light regimes (***Figure 4C,D***). Indeed, we found that even at high light irradiances HXK1 does not participate in the repression of *CAB2* and *CAA* (***Figure 4E***). It is possible that glucose-activated HXK1 signalling is more prevalent in adult plants that have increased capacity for photosynthesis and therefore potential for glucose-activated signalling. Indeed,

in addition to its proposed nuclear signalling role, a novel sucrose-dependent cytosolic function has been proposed for HXK1 involving the direct interaction with KINγ, a SUCROSE NON-FERMENTING1 (SNF1)-RELATED KINASE (SNRK1) subunit (***Van Dingenin et al., 2018***). Our study re-casts HXK1 as a catabolic enzyme that plays a central role in supporting post-germination growth. An important function of the HXK1-glycolytic pathway is to couple the metabolism transcriptome to the energy status of the seedling.

Materials and Methods

Plant material, growth conditions, and treatments. The wild-type Arabidopsis thaliana ecotypes used in this study are Landsberg *erecta* (Ler) and Columbia-0 (Col). The EMS derived HXK1 nonsense mutant allele *gin2-1* (Ler) (***Moore et al., 2003***) and SALK T-DNA insertion null allele *hxk1-3* (CS861759) (Col) (***Huang et al., 2015***) were obtained from The Nottingham Arabidopsis Stock Centre (NASC), UK. For all experiments, seeds were surface-sterilized as previously described in (***Fankhauser and Casal, 2004***), sown on 0.5X MS plates ((Duchefa Biochemie, M0221), 0.8% agar, pH 5.7) and stratified in darkness for 2-3 days at 4°C. Specific details on growth conditions are mentioned in the respective figure legends. Polylux XLR FT8/18W/835 fluorescent tubes (GE, Belgium) were used as a light source at fluence rates indicated in the respective figure legends.

Seedling hypocotyl length and cotyledon area measurements. Images of seedlings laid flat on growth media was used to quantify hypocotyl length and cotyledon area using ImageJ (NIH, Maryland) and Adobe Photoshop CS6 (Adobe, California) respectively. For glucose-6-phosphate (G6P) (Sigma G7879) and sodium pyruvate (Sigma P2256) treatments, desired concentrations from filter sterilized stocks were added to cool sterilized media and seeds directly sown. Unless otherwise stated, all experiments were performed in triplicate with 40 seedlings per replicate.

Seedling hypocotyl cell counts and length measurements. For determination of etiolated hypocotyl epidermal cell lengths/numbers, seedlings were cleared overnight as described in (***Weigel and Glazebrook, 2002***), mounted on slides and visualized using Eclipse E600 Nikon DIC microscope. Individual cell lengths from each section of the hypocotyl (basal,

middle, upper) was measured using ImageJ and cell number per file was obtained by manual count. Unless otherwise stated, all experiments were performed in triplicate with 20 seedlings per replicate.

Glucose quantification. Seedlings were harvested in liquid nitrogen, finely ground and ethanol extracted thrice. Glucose was then quantified using an enzymatic assay at 340nm wavelength and normalized to material fresh weight. The procedure has been described in detail previously (***Hendriks et al., 2003***). Unless otherwise stated, all experiments were performed in triplicate with 50 seedlings per replicate

Gene expression analysis. For qRT-PCR experiments, seedlings harvested in liquid nitrogen was ground into fine powder. Total RNA was extracted using the RNeasy Plant Mini Kit (Qiagen) with on-column DNase digestion. cDNA synthesis was performed using the qScript cDNA SuperMix (Quanta Biosciences) as described by the manufacturer. The qRT-PCR was set up as a 10µL reaction using SYBR Green (Roche) in a 384-well plate, performed with a Lightcycler 480 system (Roche). Results were analysed using the Light Cycler 480 software. The primers used in this study are listed in Supplementary file 2. Unless otherwise stated, all experiments were performed in triplicate with 50 seedlings per replicate

cDNA library preparation and high throughput sequencing. Total RNA was extracted from 4-day old etiolated Ler and *gin2* seedlings (biological duplicates of 50 seedlings per replicate) as described above. Samples were then sent to Edinburgh Genomics (University of Edinburgh, UK) for QC check and sequencing. Briefly, quality check of the samples was performed using Qubit with the broad range RNA kit (Thermo Fisher Scientific) and Tapestation 4200 with the RNA Screentape for eukaryotic RNA analysis (Agilent). Libraries were prepared using the TruSeq Stranded mRNA kit (Illumina), and then validated. Samples were pooled to create 4 multiplexed DNA libraries, which were paired-end sequenced on an Illumina HiSeq 4000 platform (Machine name K00166, Run number 346, flowcell AHT2HKBBXX, lanes 5 and 6). On average 26.6 million 150nt PE reads were obtained for each sample.

Processing of RNA sequencing reads. Sequence reads were aligned against the Arabidopsis thaliana genome (TAIR10) with TopHat v2.1.1 (***Kim et al., 2013***) with default parameters, except in the case of the maximum intron length parameter, which was set at 5000. Count tables for the different feature levels were obtained from bam files using the ASpli package version 1.6.0 (***Mancini et al. 2018***) with custom R scripts and considering the AtRTDv1 transcriptome (***Zhang et al., 2015***). Count tables at the gene level presented a good correlation overall between replicates and samples. Raw sequences (fastq files) and used in this paper have been deposited in the ArrayExpress (***Kolesnikov et al., 2015***) database at EMBL-EBI (www.ebi.ac.uk/arrayexpress) under accession number E-MTAB-7654.

Differential gene expression analysis. Differential gene expression analysis was conducted for 18,225 genes whose expression was above a minimum threshold level (read density > 0.05) in at least one experimental condition. Read density (rd) was computed as the number of reads in each gene divided by its effective width. The term effective width corresponds to the sum of the length of all the exons of a given gene. Differential gene expression was estimated using the edgeR package version 3.22.3 (***Robinson et al., 2009***) and resulting p values were adjusted using a false discovery rate (FDR) criterion. Genes with FDR values lower than 0.1 and a log2 fold change > 0.6 were considered to be differentially expressed. Heatmaps were generated using R.

Acknowledgements. A.G was supported by a University of Edinburgh Darwin Trust Scholarship. This work was funded by the Biotechnology and Biological Sciences Research Council (BBSRC)-National Science Foundation Grant BB/M025551/1 (awarded to K.J.H) and 14 ERA-CAPS PHYTOCAL Grant BB/N005147/1 (awarded to K.J.H).

References

445 **Baena-González E**, Rolland F, Thevelein JM, Sheen J. 2007. A central integrator of transcription
446 networks in plant stress and energy signalling. *Nature*. **448**:938-42.
447 **Baud S**, Dubreucq B, Miquel M, Rochat C, Lepiniec L. 2008. Storage reserve accumulation in
448 Arabidopsis: metabolic and developmental control of seed filling. *Arabidopsis Book* **6**:e0113. doi:
449 10.1199/tab.0113.
450 **Binder S.** 2010. Branched-Chain Amino Acid Metabolism in Arabidopsis thaliana. *Arabidopsis Book*.
451 **8**:e0137. doi: 10.1199/tab.0137.
452 **Cárdenas ML**, Cornish-Bowden A, Ureta T. 1998. Evolution and regulatory role of the hexokinases.
453 *Biochim Biophys Acta*. **1401**:242-64.
454 **Chaiwanon J**, Wang W, Zhu JY, Oh E, Wang ZY. 2016. Information Integration and Communication in
455 Plant Growth Regulation. *Cell* **164**:1257-1268. doi: 10.1016/j.cell.2016.01.044.
456 **Chen GH**, Liu MJ, Xiong Y, Sheen J, Wu SH. 2018. TOR and RPS6 transmit light signals to enhance
457 protein translation in deetiolating Arabidopsis seedlings. *Proc Natl Acad Sci U S A*. **115**:12823-12828.
458 doi: 10.1073/pnas.1809526115.
459 **Cho YH**, Yoo SD, Sheen J. 2006. Regulatory functions of nuclear hexokinase1 complex in glucose
460 signalling. *Cell* **127**:579-89.
461 **Claeyssen E**, Rivoal J. 2007. Isozymes of plant hexokinase: occurrence, properties and functions.
462 *Phytochemistry.* **68**:709-31.
463 **de Jong F**, Thodey K, Lejay LV, Bevan MW. 2014. Glucose elevates NITRATE TRANSPORTER2.1 protein
464 levels and nitrate transport activity independently of its HEXOKINASE1-mediated stimulation of
465 NITRATE TRANSPORTER2.1 expression. *Plant Physiol.* **164**:308-20. doi: 10.1104/pp.113.230599.
466 **Eastmond PJ**, Germain V, Lange PR, Bryce JH, Smith SM, Graham IA. 2000. Postgerminative growth
467 and lipid catabolism in oilseeds lacking the glyoxylate cycle. *Proc Natl Acad Sci U S A.* **97**:5669-74.
468 **Fankhauser C**, Casal JJ. 2004. Phenotypic characterization of a photomorphogenic mutant. *Plant J.*
469 **39**:747-60.

470 **Gommers CMM**, Monte E. 2018. Seedling Establishment: A Dimmer Switch-Regulated Process
471 between Dark and Light Signalling. *Plant Physiol.* **176**:1061-1074. doi: 10.1104/pp.17.01460.
472 **Graham IA.** 2008. Seed storage oil mobilization. *Annu Rev Plant Biol.* **59**:115-42. doi:
473 10.1146/annurev.arplant.59.032607.092938.
474 **Hashimoto T.** 2015. Microtubules in plants. *Arabidopsis Book*. **13**:e0179. doi: 10.1199/tab.0179.
475 **Hendriks JH**, Kolbe A, Gibon Y, Stitt M, Geigenberger P. 2003. ADP-glucose pyrophosphorylase is
476 activated by posttranslational redox-modification in response to light and to sugars in leaves of
477 Arabidopsis and other plant species. *Plant Physiol*. **133**:838-49.
478 **Hildebrandt TM**, Nunes Nesi A, Araújo WL, Braun HP. 2015. Amino Acid Catabolism in Plants. *Mol*
479 *Plant.* **8**:1563-79. doi: 10.1016/j.molp.2015.09.005.
480 **Hornitschek P**, Kohnen MV, Lorrain S, Rougemont J, Ljung K, López-Vidriero I, Franco-Zorrilla JM,
481 Solano R, Trevisan M, Pradervand S, Xenarios I, Fankhauser C. 2012. Phytochrome interacting factors
482 4 and 5 control seedling growth in changing light conditions by directly controlling auxin signalling.
483 *Plant J.* **71**:699-711. doi: 10.1111/j.1365-313X.2012.05033.x.
484 **Hsu YF**, Chen YC, Hsiao YC, Wang BJ, Lin SY, Cheng WH, Jauh GY, Harada JJ, Wang CS. 2014. AtRH57,
485 a DEAD-box RNA helicase, is involved in feedback inhibition of glucose-mediated abscisic acid
486 accumulation during seedling development and additively affects pre-ribosomal RNA processing with
487 high glucose. *Plant J.* **77**:119-35. doi: 10.1111/tpj.12371.
488 **Huang JP**, Tunc-Ozdemir M, Chang Y, Jones AM. 2015. Cooperative control between AtRGS1 and
489 AtHXK1 in a WD40-repeat protein pathway in Arabidopsis thaliana. *Front Plant Sci.* **6**:851. doi:
490 10.3389/fpls.2015.00851.
491 **Kelly G**, Sade N, Doron-Faigenboim A, Lerner S, Shatil-Cohen A, Yeselson Y, Egbaria A, Kottapalli J,
492 Schaffer AA, Moshelion M, Granot D. 2017. Sugar and hexokinase suppress expression of PIP
493 aquaporins and reduce leaf hydraulics that preserves leaf water potential. *Plant J.* **91**:325-339. doi:
494 10.1111/tpj.13568.

495 **Kim D**, Pertea G, Trapnell C, Pimentel H, Kelley R, Salzberg SL. 2013. TopHat2: accurate alignment of
496 transcriptomes in the presence of insertions, deletions and gene fusions. *Genome Biol.* **14:**R36. doi:
497 10.1186/gb-2013-14-4-r36.
498 **Kolesnikov N**, Hastings E, Keays M, Melnichuk O, Tang YA, Williams E, Dylag M, Kurbatova N,
499 Brandizi M, Burdett T, Megy K, Pilicheva E, Rustici G, Tikhonov A, Parkinson H, Petryszak R, Sarkans
500 U, Brazma A. 2015. ArrayExpress update--simplifying data submissions. *Nucleic Acids Res*. **43**:D1113-
501 6. doi:10.1093/nar/gku1057
502 **Kunz S**, Gardeström P, Pesquet E, Kleczkowski LA. 2015. Hexokinase 1 is required for glucose-
503 induced repression of bZIP63, At5g22920, and BT2 in Arabidopsis. *Front Plant Sci.* **6**:525. doi:
504 10.3389/fpls.2015.00525
505 **Leivar P**, Monte E, Oka Y, Liu T, Carle C, Castillon A, Huq E, Quail PH. 2008. Multiple phytochrome-
506 interacting bHLH transcription factors repress premature seedling photomorphogenesis in darkness.
507 *Curr Biol.* **18**:1815-23. doi: 10.1016/j.cub.2008.
508 **Leivar P**, Monte E. 2014. PIFs: systems integrators in plant development. *Plant Cell.* **26**:56-78. doi:
509 10.1105/tpc.113.120857.
510 **Leivar P**, Tepperman JM, Cohn MM, Monte E, Al-Sady B, Erickson E, Quail PH. 2012. Dynamic
511 antagonism between phytochromes and PIF family basic helix-loop-helix factors induces selective
512 reciprocal responses to light and shade in a rapidly responsive transcriptional network in
513 Arabidopsis. *Plant Cell*. **24**:1398-419. doi: 10.1105/tpc.112.095711.
514 **Mancini E**, Iserte J, Yanovsky M, Chernomoretz A. 2018. ASpli: Analysis of alternative splicing using
515 RNA-Seq. R package version 1.6.0.
516 **Mengin V**, Pyl ET, Alexandre Moraes T, Sulpice R, Krohn N, Encke B, Stitt M. 2017. Photosynthate
517 partitioning to starch in Arabidopsis thaliana is insensitive to light intensity but sensitive to
518 photoperiod due to a restriction on growth in the light in short photoperiods. *Plant Cell Environ.*
519 **40**:2608-2627. doi:10.1111/pce.13000.

520 **Moore B**, Zhou L, Rolland F, Hall Q, Cheng WH, Liu YX, Hwang I, Jones T, Sheen J. 2003. Role of the
521 Arabidopsis glucose sensor HXK1 in nutrient, light, and hormonal signalling. *Science*. **300**:332-6.
522 **Pedrotti L,** Weiste C, Nägele T, Wolf E, Lorenzin F, Dietrich K, Mair A, Weckwerth W, Teige M, Baena-
523 González E, Dröge-Laser W. 2018. Snf1-RELATED KINASE1-Controlled C/S1-bZIP Signalling Activates
524 Alternative Mitochondrial Metabolic Pathways to Ensure Plant Survival in Extended Darkness. *Plant*
525 *Cell* **30**:495-509. doi: 10.1105/tpc.17.00414.
526 **Penfield S**, Pinfield-Wells HM, Graham IA. 2006. Storage reserve mobilisation and seedling
527 establishment in Arabidopsis. *Arabidopsis Book* **4**:e0100. doi:10.1199/tab.0100.
528 **Penfield S**, Rylott EL, Gilday AD, Graham S, Larson TR, Graham IA. 2004. Reserve mobilization in the
529 Arabidopsis endosperm fuels hypocotyl elongation in the dark, is independent of abscisic acid, and
530 requires PHOSPHOENOLPYRUVATE CARBOXYKINASE1. *Plant Cell*. **16**:2705-18.
531 **Pfeiffer A**, Shi H, Tepperman JM, Zhang Y, Quail PH. 2014. Combinatorial complexity in a
532 transcriptionally centered signalling hub in Arabidopsis. *Mol Plant.* **7**:1598-1618. doi:
533 10.1093/mp/ssu087.
534 **Price J**, Laxmi A, St Martin SK, Jang JC. 2004. Global transcription profiling reveals multiple sugar
535 signal transduction mechanisms in Arabidopsis. *Plant Cell.* **16**:2128-50.
536 **Robinson MD**, McCarthy DJ, Smyth GK. 2010. edgeR: a Bioconductor package for differential
537 expression analysis of digital gene expression data. *Bioinformatics*. **26**:139-40. doi:
538 10.1093/bioinformatics/btp616.
539 **Simon NML,** Kusakina J, Fernández-López Á, Chembath A, Belbin FE, Dodd AN. 2018. The Energy-
540 Signalling Hub SnRK1 Is Important for Sucrose-Induced Hypocotyl Elongation. *Plant Physiol.*
541 **176**:1299-1310. doi: 10.1104/pp.17.01395.
542 **Singh M**, Gupta A, Singh D, Khurana JP, Laxmi A. 2017. Arabidopsis RSS1 Mediates Cross-Talk
543 Between Glucose and Light Signalling During Hypocotyl Elongation Growth. *Sci Rep.* **7**:16101. doi:
544 10.1038/s41598-017-16239-y.

545 **Stewart JL**, Maloof JN, Nemhauser JL. 2011. PIF genes mediate the effect of sucrose on seedling
546 growth dynamics. *PLoS One*. **6**:e19894. doi:10.1371/journal.pone.0019894.
547 **Theodoulou FL**, Eastmond PJ. 2012. Seed storage oil catabolism: a story of give and take. *Curr Opin*
548 *Plant Biol.* **15**:322-8. doi: 10.1016/j.pbi.2012.03.017.
549 **Ulfstedt M**, Hu GZ, Eklund DM, Ronne H. 2018. The Ability of a Charophyte Alga Hexokinase to
550 Restore Glucose Signalling and Glucose Repression of Gene Expression in a Glucose-Insensitive
551 Arabidopsis Hexokinase Mutant Depends on Its Catalytic Activity. *Front Plant Sci.* **9**:1887. doi:
552 10.3389/fpls.2018.01887.
553 **Van Dingenen J**, Vermeersch M, De Milde L, Hulsmans S, De Winne N, Van Leene J, Gonzalez N,
554 Dhondt S, De Jaeger G, Rolland F, Inzé D. 2019. The role of HEXOKINASE1 in Arabidopsis leaf growth.
555 *Plant Mol Biol.* **99**:79-93. doi: 10.1007/s11103-018-0803-0
556 **Weigel D** & Glazebrook J. 2002. Arabidopsis: A Laboratory Manual (Cold Spring Harbor Laboratory
557 Press, Cold Spring Harbor, NY).
558 **Yanagisawa S**, Yoo SD, Sheen J. 2003. Differential regulation of EIN3 stability by glucose and
559 ethylene signalling in plants. *Nature* **425**:521-5.
560 **Yang L**, Xu M, Koo Y, He J, Poethig RS. 2013. Sugar promotes vegetative phase change in Arabidopsis
561 thaliana by repressing the expression of MIR156A and MIR156C. *Elife.* **26**;2:e00260. doi:
562 10.7554/eLife.00260
563 **Yu S**, Cao L, Zhou CM, Zhang TQ, Lian H, Sun Y, Wu J, Huang J, Wang G, Wang JW. 2013. Sugar is an
564 endogenous cue for juvenile-to-adult phase transition in plants. *Elife*. **26**;2:e00269. doi:
565 10.7554/eLife.00269
566 **Zhang R,** Calixto CP, Tzioutziou NA, James AB, Simpson CG, Guo W, Marquez Y, Kalyna M, Patro R,
567 Eyras E, Barta A, Nimmo HG, Brown JW. 2015. AtRTD - a comprehensive reference transcript dataset
568 resource for accurate quantification of transcript-specific expression in Arabidopsis thaliana. *New*
569 *Phytol*. **208**:96-101. doi: 10.1111/nph.13545.

570 **Zhang Y**, Mayba O, Pfeiffer A, Shi H, Tepperman JM, Speed TP, Quail PH. 2013. A quartet of PIF bHLH
571 factors provides a transcriptionally centered signalling hub that regulates seedling morphogenesis
572 through differential expression-patterning of shared target genes in Arabidopsis. *PLoS Genet.*
573 **9**:e1003244. doi: 10.1371/journal.pgen.1003244.
574 **Zhang Z**, Zhu JY, Roh J, Marchive C, Kim SK, Meyer C, Sun Y, Wang W, Wang ZY. 2016. TOR Signalling
575 Promotes Accumulation of BZR1 to Balance Growth with Carbon Availability in Arabidopsis. *Curr Biol.*
576 **26:**1854-60. doi:10.1016/j.cub.2016.05.005.
577 **Zhang ZW**, Yuan S, Xu F, Yang H, Zhang NH, Cheng J, Lin HH. 2010. The plastid hexokinase pHXK: a
578 node of convergence for sugar and plastid signals in Arabidopsis. *FEBS Lett.* **584**:3573-9. doi:
579 10.1016/j.febslet.2010.07.024.
580
581
582
583
584
585
586
587
588

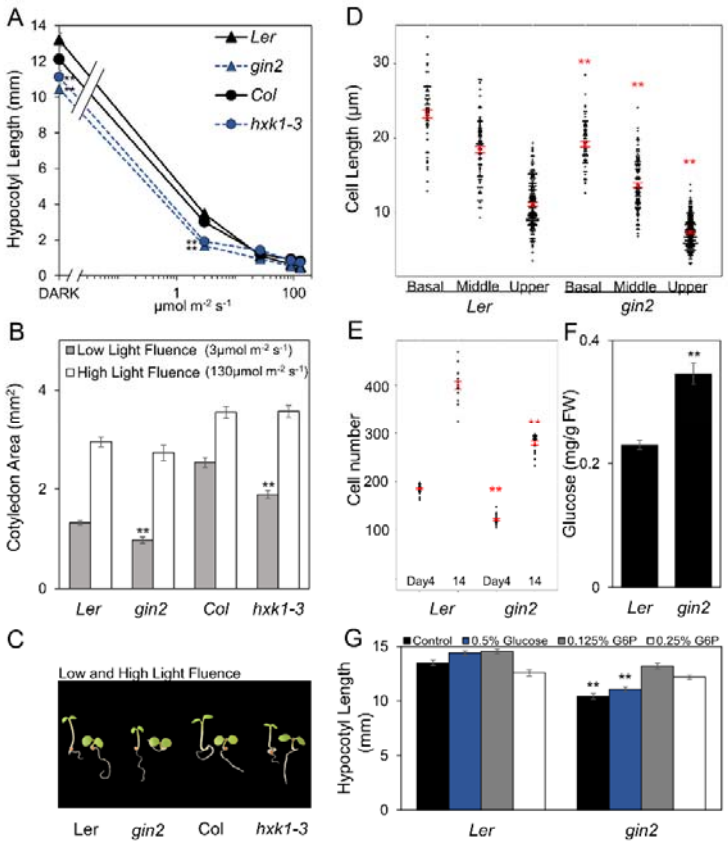

Figure 1. HXK1 operates in the dark and low light during seedling development. (**A)** Fluence rate response curves for hypocotyl elongation in 7 day old WT, *gin2* (Ler) and *hxk1-3* (Col) seedlings grown in continuous light at 18°C. Cotyledon area (**B**) and images of seedlings (**C**) grown in low or high light (3 or 130 µmol m^{-2} s^{-1}). (**D**) Epidermal cell length at the basal, middle and upper regions of hypocotyl in etiolated WT (Ler) and *gin2* seedlings at 4 days. (**E**) Hypocotyl epidermal cell number in etiolated WT (Ler) and *gin2* seedlings at 4 and 14 days. Red circles in the dot plots indicate mean value. (**F**) Glucose content (mg/g FW) in 4 day old etiolated WT (Ler) and *gin2* seedlings. (**G**) Hypocotyl length of etiolated 7 day old WT (Ler) and *gin2* seedlings grown at 18°C without or with 0.5% (w/v) glucose, 0.125% and 0.25% (w/v) G6P. Error bars indicate ±SEM; **P ≤ 0.01 (Student's t-test) of mutants relative to respective WT for each condition.

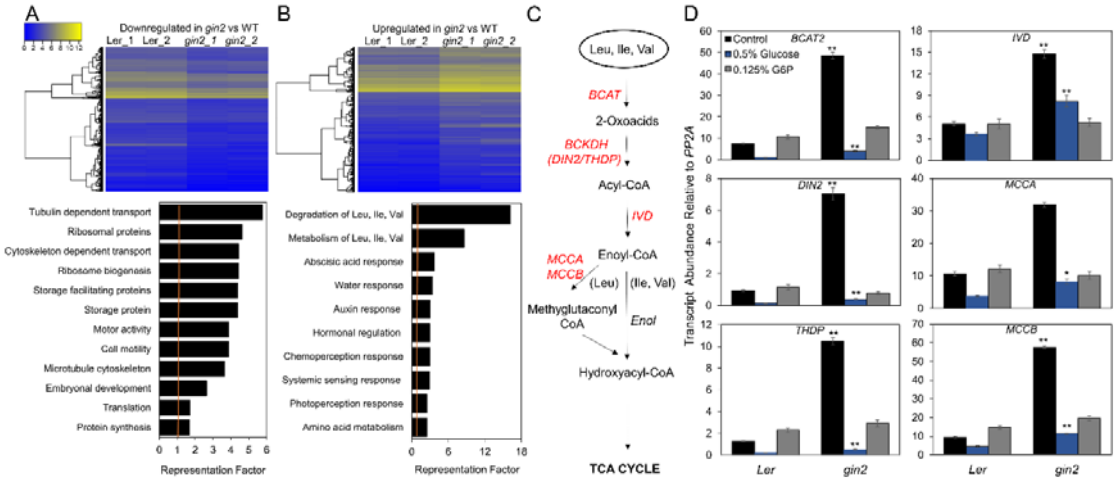

Figure 2. HXK1 regulates key energy regulated pathways**.** Hierarchical clustering and Gene Ontology analysis of (**A**) upregulated and (**B**) downregulated genes in etiolated WT (Ler) and *gin2* biological duplicates at 4 days. Scale bar denotes log counts per million, low (blue) to high (yellow). Bar plots of statistically significant (p≤0.01, Fisher Exact Test) GO terms derived from VirtualPlant database; orange line denotes an observed:expected frequency ratio of 1. (**C**) Branched Chain Amino Acid (BCAA) degradation pathway schematic with enzymes upregulated in *gin2* highlighted in red. (**D**) Transcript abundance (qPCR) of BCAA pathway genes in 4 day old etiolated WT (Ler) and *gin2* seedlings grown at 18°C with or without 0.5% w/v glucose or 0.125% w/v G6P. Error bars indicate ±SE, *P ≤ 0.05, **P≤ 0.01 (Student's t-test) of *gin2* relative to WT for each treatment.

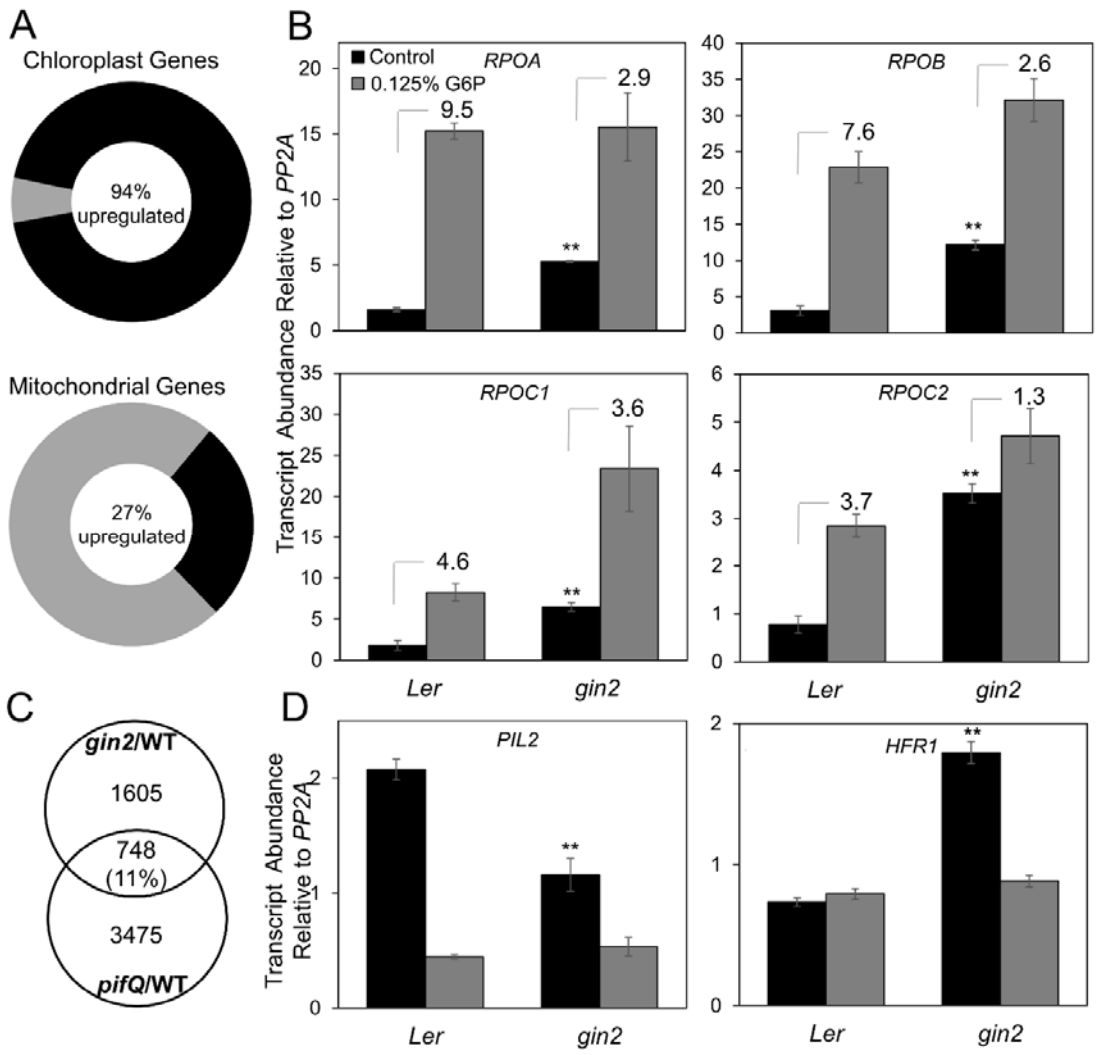

Figure 3. HXK1 represses plastome genes and operates mainly independently of PIFs during skotomorphogenesis. (**A**) Proportion of upregulated chloroplast and mitochondrial genes (from RNAseq) in etiolated *gin2* seedlings relative to WT (Ler) at 4 days. (**B**) Transcript abundance (qPCR) of plastid encoded polymerases (RPOs) in 4 day old etiolated WT (Ler) and *gin2* seedlings grown at 18ºC without or with 0.125% w/v G6P. Fold change induced by treatment is shown. (**C**) Comparison of *gin2*/WT and *pifQ*/WT transcriptomes from etiolated seedlings (**Pfeiffer et al., 2014**). (**D**) *PIL2* and *HFR1* transcript abundance (qPCR) in 4 day old etiolated WT (Ler) and *gin2* seedlings grown at 18ºC without or with 0.125% w/v G6P. Error bars indicate ±SE, **P≤ 0.01 (Student's t-test) of *gin2* relative to WT (Ler) for each treatment.

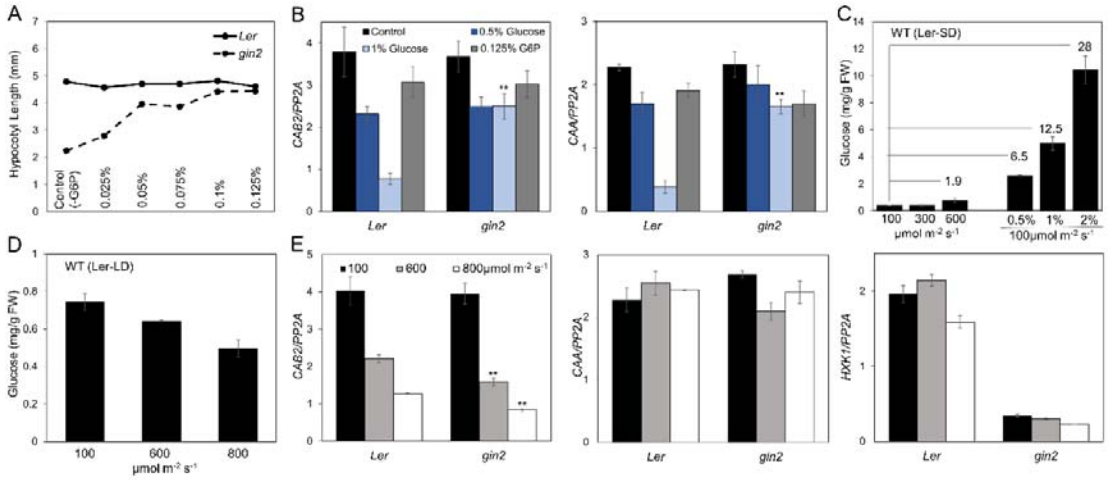

Figure 4. HXK1 does not control *CAB2* or *CAA* expression under physiological conditions. (**A**) Hypocotyl length of 7 day old WT (Ler) and *gin2* seedlings grown in low light (3µmol m^{-2} s^{-1}) at 18ºC without or with increasing concentrations of G6P. (**B**) Transcript abundance of *CAB2* and *CAA* in WT (Ler) and *gin2* seedlings grown in 100µmol m^{-2} s^{-1} light, without or with 0.5%, 1% w/v glucose, or 0.125% w/v G6P. (**C**) Glucose (mg/g FW) levels in WT (Ler) seedlings grown at increasing light intensities (100, 300 and 600µmol m^{-2} s^{-1}) or at 100µmol m^{-2} s^{-1} plus increasing concentrations of exogenous glucose (0%, 0.5%, 1% and 2% (w/v)). For both (**B**) and (**C**) seedlings were grown in SD photoperiods at 18°C and sampled on day 4 at ZT4. (**D**) WT (Ler) Glucose (mg/g FW) levels at increasing light intensities (100, 600 and 800µmol m^{-2} s^{-1}). (**E**) *HXK1*, *CAA* and *CAB2* transcript abundance (qPCR) in Ler and *gin2* seedlings grown at increasing light intensities. For both (**D**) and (**E**) seedlings were grown in LD photoperiods at 22°C and sampled after 7 days at EoD (ZT16). Error bars indicate ±SE, **P≤ 0.01 (Student's t-test) of *gin2* relative to WT (Ler) for each treatment.

Supplementary Information

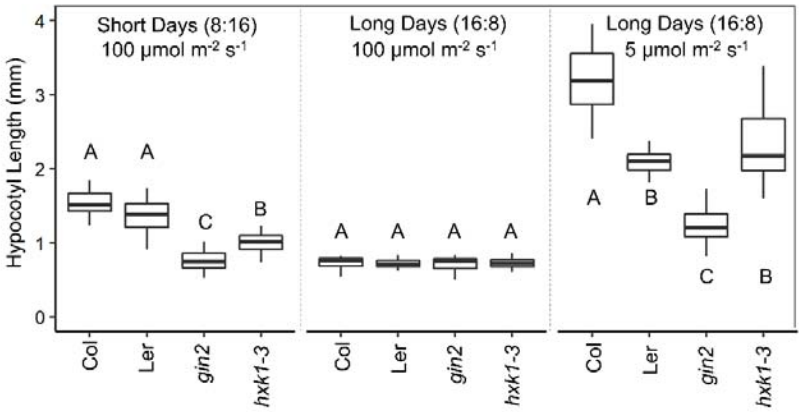

Figure 1–figure supplement 1. HXK1 operates in the dark and suboptimal light during seedling establishment. Hypocotyl length of 7-day old WT, *gin2* (Ler) and *hxk1-3* (Col) seedlings grown in Short Day (SD) and long day (LD) photoperiods at 100µmol $m^{-2}s^{-1}$ or in LD at 5µmol $m^{-2}s^{-1}$ light at 18°C. Horizontal bars, boxes, and whiskers show medians, interquartile ranges (IQR), and data ranges, respectively. Different letters denote statistical differences ($P > 0.05$) among samples as assessed by one-factorial ANOVA and Tukey HSD.

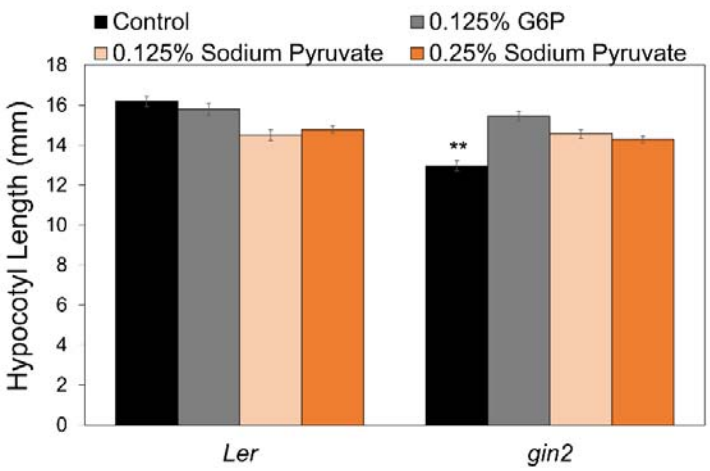

Figure 1-figure supplement 2. Hypocotyl length of 7 day old etiolated WT (Ler) and *gin2* seedlings grown in the absence and presence of 0.125% G6P, 0.125% and 0.25% (w/v) sodium pyruvate at 18°C. Error bars indicate ±SE, **P≤ 0.01 (Student's *t*-test) of *gin2* relative to WT (Ler) for each treatment.

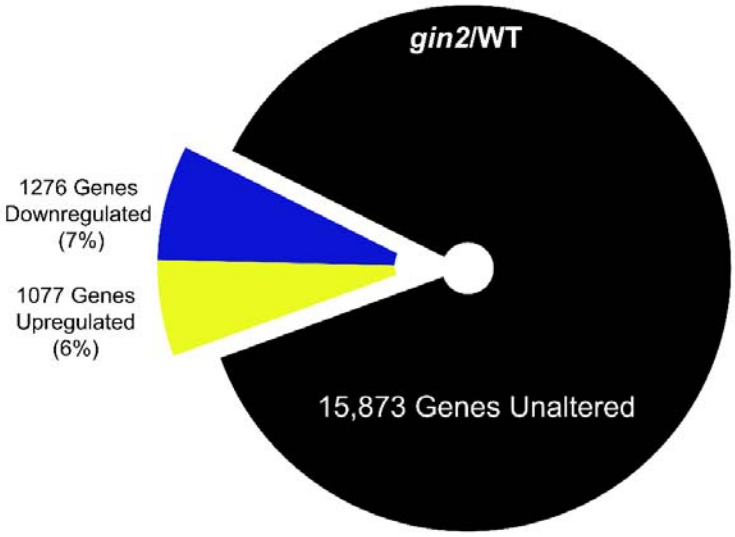

Figure 2-figure supplement 1. Percentage of genes down and up-regulated (± 1.5 FC) in 4 day old etiolated *gin2* vs WT (Ler).

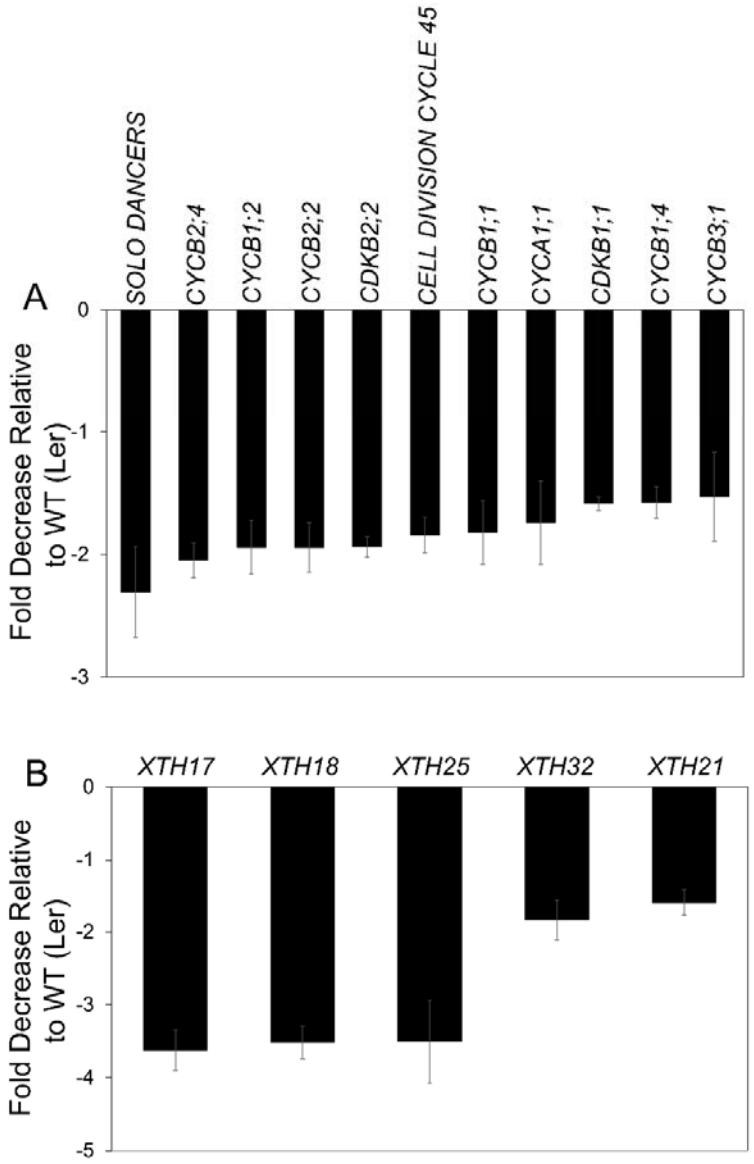

Figure 2-figure supplement 2. Fold decrease of (**A**) core cell cycle/cell division genes, (**B**) cell wall modifying XYLOGLUCOSYL TRANSFERASE (XTH) genes in *gin2* relative to WT (Ler) derived from the RNAseq experiment. Error bars represent the propagated error value.

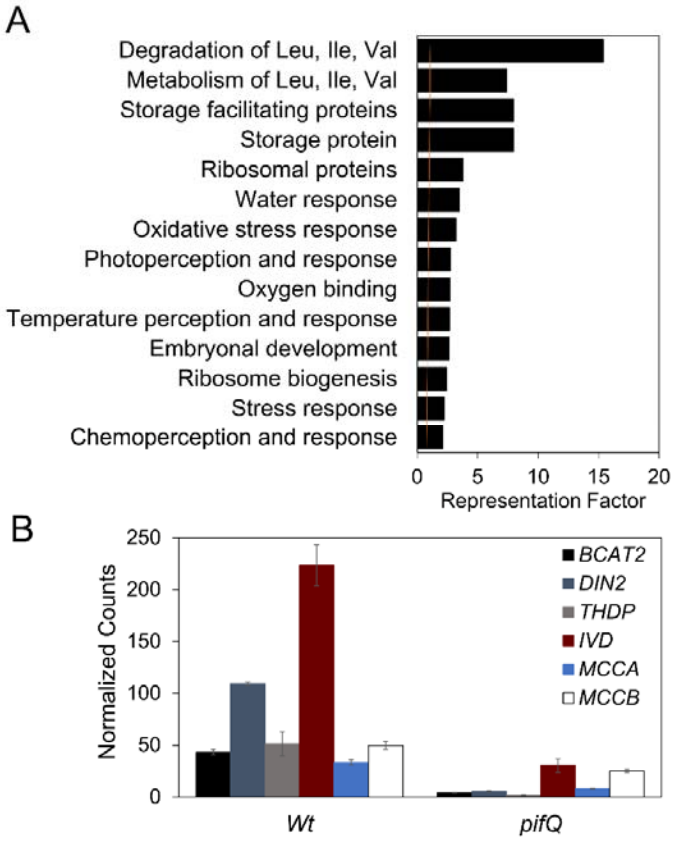

Figure 3-figure supplement 1. HXK1 and PIFs largely operate independently during skotomorphogenesis. **(A)** Statistically significant ($p \leq 0.01$, Fisher Exact Test) GO terms derived from VirtualPlant database for 748 overlapping genes mis-regulated in the *gin2* and *pifQ* mutant are plotted. Orange line indicate representation factor of 1 (observed/expected frequency ratio). **(B)** Normalised counts for BCAA catabolic genes in WT and *pifQ* (Raw RNAseq data derived from ***Zhang et al., 2013***).

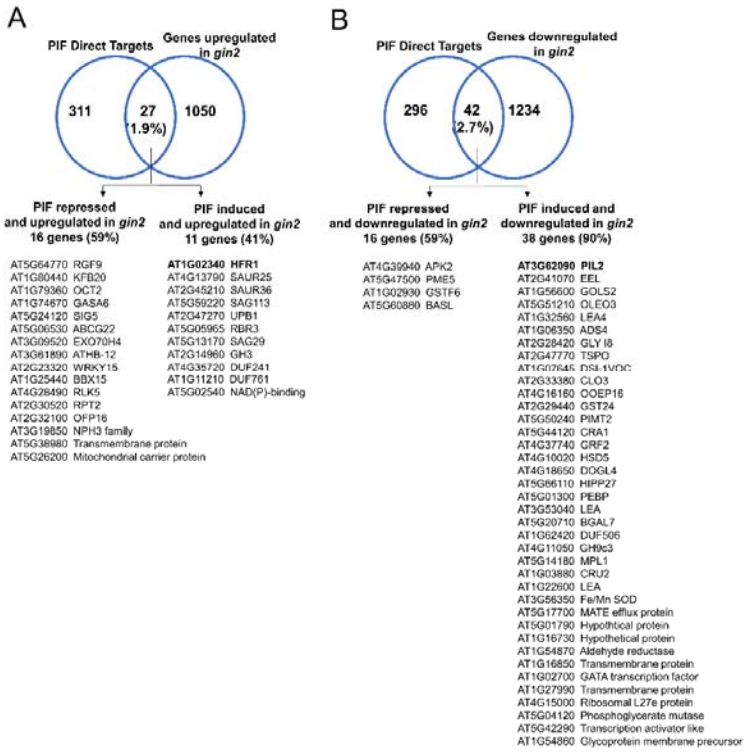

Figure 3-figure supplement 2. HXK1 and PIFs largely operate independently during skotomorphogenesis. Comparison between direct PIF targets (data derived from ***Pfeiffer et al., 2014***) with genes **(A)** upregulated and **(B)** downregulated in *gin2*. Genes regulated in a similar or opposite manner are depicted below venn diagrams.

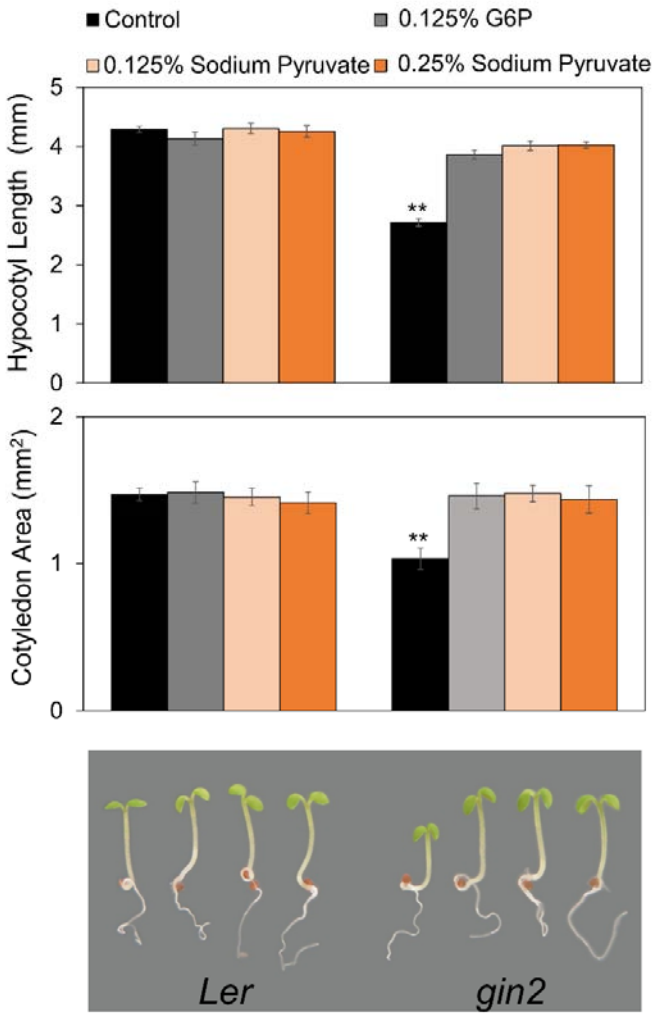

674

675 **Figure 4-figure supplement 1.** Restoring energy recues the *gin2* mutant seedling phenotype in low
676 light. **(A)** Hypocotyl length and **(B)** cotyledon area of 7 day old WT (Ler) and *gin2* seedlings grown in
677 the absence and presence of 0.125% w/v G6P and 0.125% and 0.25% (w/v) sodium pyruvate under
678 continuous low light (3μmol m^{-2} s^{-1}) conditions at 18°C. Error bars indicate ±SE, **P≤ 0.01 (Student's
679 *t*-test) of *gin2* relative to WT (Ler) for each treatmen

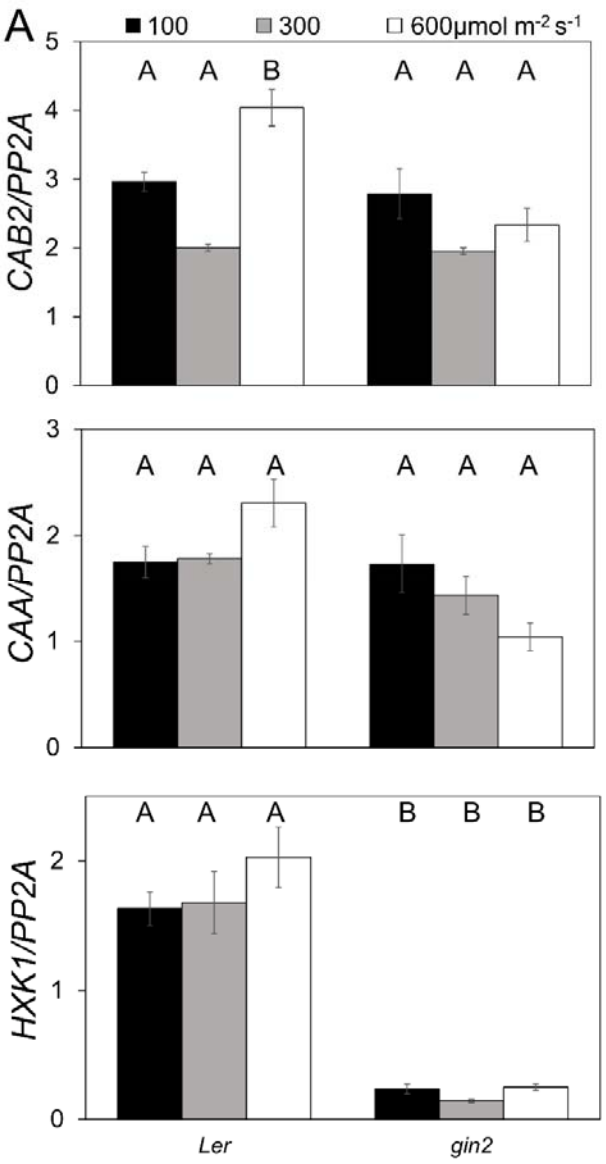

Figure 4-figure supplement 2. Photosynthetic feedback inhibition mediated by HXK1 signalling does not occur in seedlings. qPCR measuring *CAB2*, *CAA* and *HXK1* transcript abundance at ZT4 in 4 day old WT (Ler) and *gin2* seedlings grown under increasing light intensities (100, 300 and 600µmol m^{-2} s^{-1}) in SD photoperiods at18°C. Different letters denote statistical differences ($P > 0.05$) among samples as assessed by one-factorial ANOVA and Tukey HSD.

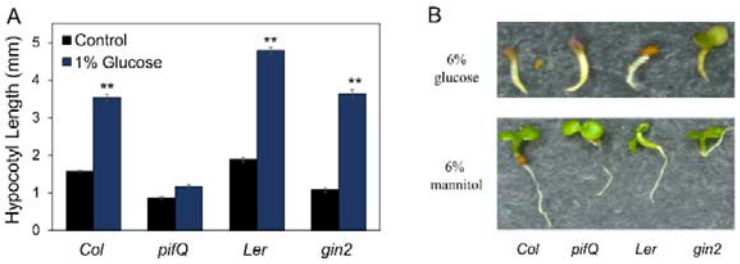

Supplement figure 1. HXK1 and PIFs operate in independent sugar signalling pathways. (*A*) Hypocotyl length of 7 day old WT, *pifQ* (Col) and *gin2* (Ler) seedlings grown in short days (100µmol m^{-2} s^{-1}) in the absence (black bar) and presence of 1% (w/v) glucose at 18°C. (*B*) Images of 7 day old seedlings grown under continuous light (130µmol m^{-2} s^{-1}) in the presence of 6% (w/v) glucose or mannitol at 18°C. Error bars indicate ±SE, **P≤ 0.01 (Student's *t*-test) of glucose treated relative to untreated

Supplement figure 2. Primers used in this work.

Primer name	Sequence (5'-3')
AG_2250_RPOA_F	GCGATGCGAAGAGCTTTACT
AG_2251_RPOA_R	CCAGGACCTTGGACACAAA
AG_2252_RPOB_F	GATGTGAGGTGGGTTCAGAA
AG_2253_RPOB_R	GGTCTCCCGTCTTGCAAATA
AG_2254_RPOC1_F	TTCTTCCTCCCGAGTTGAGA
AG_2255_RPOC1_R	CCACGGCTTCTTGTACCAAT
AG_2256_RPOC2_F	CGCGTCGACTTGTTGAAGTA
AG_2257_RPOC2_R	CGTCTGCTAAGACACGACCA
AG_2236_BCAT2_F	GGGATAATCTCGGGTTTGGT
AG_2237_BCAT2_R	CTTCATCCGGATAGCGTTGT
AG_2232_THDP_F	GACGAAGACGGACGAATCAT

AG_2233_THDP_R	TGCTGAAGCGATGTTAATGG
AG_2234_DIN2_F	CGGTCGTCGGAGAGAGTAAC
AG_2235_DIN2_R	GCCTTGCAAAACACCAAAAT
AG_2238_MCCA_F	CCCGTCTACAGGTCGAACAT
AG_2239_MCCA_R	ACCCGAACTGATGGTGAGAC
AG_2240_IVD_F_	ACTCTGTTGCGAGGGACTGT
AG_2241_IVD_R	CTTAGAAGGCGTCCTGTTGC
AG_2242_MCCB_F	CTTTGCCTTCAGGTGGGATA
AG_2243_MCCB_R	ACCGAGCAGCAATCTCTTGT
AG_1267_CAB2_F	CCCTGGAGACTACGGATG
AG_1267_CAB2_R	TCCAAACTTGACTCCGTTCC
AG_1428_CAA_F	TGAATACGCTGTCTTGCACC
AG_1429_CAA_R	TGTGATGGTGGTGGTAGCGA
DY_1166_HXK1_F	GGTTTCACTTTCTCGTTTCCTG
DY_1167_HXK1_R	CTTGTCCAACTGCTTCTTCG

Figure 2—source data 1

List of genes altered in 4-day-old etiolated *gin2* mutants

HXK1 regulated genes were defined by 1.5-fold difference between *gin2* and WT (Ler) with $p<0.01$.